accepted for publication in: ASME Journal of Heat Transfer, Sept 2015

Identification of the Thermophysical Properties of the Soil by Inverse Problem

Salwa Mansour
PhD student, INRIA
Campus de Beaulieu, Rennes (FR)
Email: salwa.mansour@inria.fr

Édouard Canot
CNRS researcher, IRISA
Campus de Beaulieu, Rennes (FR)
Email: edouard.canot@irisa.fr

Mohamad Muhieddine
Assistant professor, Lebanese University
Nabatieh campus section V (Lb)
Email: mohamad.muhieddine@liu.edu.lb

This paper introduces a numerical strategy to estimate the thermophysical properties of a saturated porous medium (volumetric heat capacity $(\rho C)_s$, thermal conductivity λ_s and porosity ϕ) where a phase change problem (liquid/vapor) appears due strong heating. The estimation of these properties is done by inverse problem knowing the heating curves at selected points of the medium. To solve the inverse problem, we use both the Damped Gauss Newton and the Levenberg Marquardt methods to deal with high nonlinearity of the system and to tackle the problem with large residuals. We use the method of lines, where time and space discretizations are considered separately. Special attention has been paid to the choice of the regularization parameter of the Apparent Heat Capacity method which may prevent the convergence of the inverse problem.

Keywords: *Thermophysical properties, Heat transfer, Porous medium, Numerical method, Inverse problem.*

1 Introduction

The work presented in this paper is motivated by the studies of agricultural and archaeological soils. A systematic application of numerical modeling in a particular field of agriculture and archaeology which is the study of seed germination and archaeological hearths is presented. The authors introduce a numerical strategy in 1D to estimate the thermophysical properties of the soil (volumetric heat capacity $(\rho C)_s$, thermal conductivity λ_s and porosity ϕ) of a saturated porous medium where a phase change problem (liquid/vapor) appears due to intense heating from above. Usually ϕ is the true porosity, however when the soil is not saturated (which should concern most cases), ϕ may be taken equal to the part of water in the pores. This is of course an approximation which is correct for the energy balance but which neglects the capillary forces and the migration flow of the liquid inside the porous media; a complete model of such an unsaturated model is out of the scope of this paper.

The investigation of the thermal properties of the soil can have significant practical consequences such as evaluation of optimum conditions for plant growth and development and can be utilized for the control of thermal-moisture regime of soil in the field [1]. These properties influence how energy is partitioned in the soil profile so the ability to monitor them is a tool to manage the soil temperature regime that affects seed germination and growth. It can also provide information about the use of fire by ancient civilizations whether for cooking or heating. The inverse problem, presented in this paper, consists of the estimation of thermophysical properties of the soil knowing the heating history curves at selected points of the altered soil [2]. In general, the mathematical formulation of inverse problems leads to models that are typically ill-posed [3]. In such problems, we usually minimize a discrepancy between some experimental data and some model data [4]. In our problem, we use the least square criterion in which the sensitivity coefficients appear and where we try to minimize the discrepancy function which is expressed as the norm of the difference between the experimental temperature and the numerical data obtained by our approximated model [5]. The system composed of the energy equation together with three boundary initial problems resulting from differentiating the basic energy equation with respect to the three unknown parameters must be solved [6].

At the stage of numerical computations, the Damped Gauss Newton method is used to minimize the least square criterion; that requires the solution of a system of four highly nonlinear ordinary differential equations. We propose a global approach similar to that presented by [2] using also the apparent heat capacity method to deal with the phase change problem. It is important to note that in our new configuration, the solution is reached after taking into consideration the temperature history at selected points of the domain and

at different time steps which was not the case in [2] where the authors reached the solution by taking the temperature history at the final time only and at all the points in the computational domain. This approach is based on the method of lines, where time and space discretizations are considered separately. The space discretization is done using a vertex-centered finite volume method; the discretization in time is done via an ODE solver that uses a BDF scheme and a modified Newton method to deal with the high nonlinearity. The code validation stage is based on the comparison between the numerical results and the synthetic data. The advantage of our configuration to that presented by [2] is that we propose a model which is more realistic and closer to the experimental setup i.e. our synthetic data consists of the calculation of the temperature at few sensors (around 5) during the whole heating duration.

2 Forward problem

The physical problem consists of heating the soil by a fire. To model this problem, we replace the soil by a perfect porous medium in 1D finite domain of length $l = 10\,cm$ with constant and uniform properties heated from above by a constant temperature T_c (temperature of the fire between 300°C and 700°C). T_c must be greater than T_v (the evaporation or phase change temperature which is normally 100°C). In the numerical examples presented in this work $T_c = 300$°C. In order to model the heat conduction transfer in the soil, we use the energy equation and we neglect the convection term so that the energy conservation equation for the unknown temperature T is expressed as:

$$(\rho C)_e \frac{\partial T}{\partial t} = \mathrm{div}\,(\lambda_e \nabla T) \tag{1}$$

with the following initial and boundary conditions:

$$T(x,0) = T_0 \text{ in } \Omega$$

$$\text{At } x = 0: \quad T(x,t) = T_c \quad \text{for } t \in (0, t_{end}] \text{ (Dirichlet)}$$

$$\text{At } x = l: \quad \frac{\partial T}{\partial x} = 0 \quad \text{for } t \in (0, t_{end}] \text{ (Neumann)}$$

where T represents the temperature, T_0 is the initial temperature at $t_0 = 0$ ($T_0 = 20$°C), T_c is the fire temperature; ρ is the density, C is the specific heat capacity, λ is the thermal conductivity, ϕ is the porosity ($\phi = 0.2$ in all what follows), the subscripts e, f and s indicate the equivalent parameters of the medium, the properties of the fluid and the porous matrix properties respectively. Note that the thermophysical properties of the fluid are temperature dependent and that is why the problem is highly nonlinear.

The effective volumetric heat capacity and the effective conductivity are defined by the equations:

$$(\rho C)_e = \phi(\rho C)_f + (1-\phi)(\rho C)_s \tag{2}$$

$$\frac{1}{\lambda_e} = \frac{\phi}{\lambda_f} + \frac{1-\phi}{\lambda_s} \tag{3}$$

Note that $(\rho C)_f = \rho_f C_f$ where ρ_f and C_f are defined as in equations 8 and 6 respectively. $(\rho C)_s = \rho_s C_s$ where the thermophysical properties of the solid matrix are that of the clay ($\rho_s = 1500\,kg/m^3$, $C_s = 1300\,J/kgK$ and $\lambda_s = 0.756\,J/kg$). The effective conductivity in equation (3) is calculated using the harmonic mean to test the algorithm. In real situations, the harmonic mean should be replaced by some other models.

To avoid the tracking of the interface of the phase change problem (liquid/vapor) which appears when the water existing in the soil turns into gas, the Apparent Heat Capacity (AHC) method is used because it allows a continuous treatment of a system involving phase transfer. The AHC method is explained in [7], where the authors showed how the singularity presented in the formulation of the thermo-physical properties defined by [8] can be treated as mentioned in [9]. The Dirac delta function, representing the equivalent heat capacity, can be approximated by the normal distribution:

$$\frac{d\sigma}{dT} = \frac{\varepsilon}{\sqrt{\pi}} exp\left[-\varepsilon^2 (T - T_v)^2\right] \tag{4}$$

where $\varepsilon = \frac{\sqrt{2}}{\Delta T}$ and T_v is the phase change temperature. ΔT is the phase change temperature interval and its choice has a strong effect on the accuracy of the AHC method. The integration of equation (4) yields the error function approximations for the initial phase fraction.

$$\sigma(T) = \frac{1}{2}\left[1 + erf(\varepsilon(T - T_v))\right] \tag{5}$$

The functions defined by equations (4) and (5) are used in the smoothing of the thermo-physical properties as shown in equations (6), (7) and (8).

$$C_f = C_l + (C_v - C_l)\sigma + L\frac{d\sigma}{dT} \tag{6}$$

$$\lambda_f = \lambda_l + (\lambda_v - \lambda_l)\sigma \tag{7}$$

$$\rho_f = \rho_l + (\rho_v - \rho_l)\sigma \tag{8}$$

where L is the latent heat of evaporation of liquid water ($L = 2.256 \times 10^6\,J/kg$) and the subscripts l and v indicate respectively the properties of the liquid water and that of the water vapor at 100°C ($\rho_l = 1000\,kg/m^3$, $C_l = 4000\,J/kgK$, $\lambda_l = 0.6\,J/kg$, $\rho_v = 0.8\,kg/m^3$, $C_v = 2000\,J/kgK$ and $\lambda_v = 2.5 \times 10^{-2}\,J/kg$).

2.1 Choice of ΔT

As previously mentioned, the choice of the value of the phase change temperature interval ΔT has a big influence on the accuracy of the solution of the heat equation. The temperature history over two sensors is shown in figure 1. The reference solution is obtained by running the forward problem with 6000 mesh cells. It seems reasonable to state

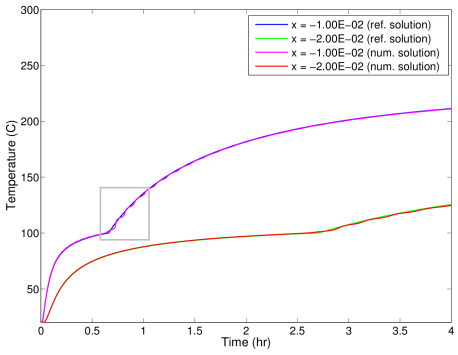

Fig. 1. Temperature history for $\Delta T = \Delta T_{optimum}$ and for 160 mesh cells. Comparison between numerical and reference solutions.

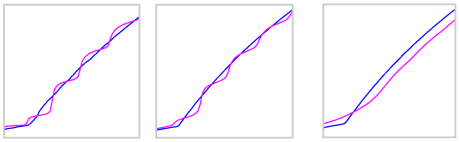

Fig. 2. The zoom of temperature history near the phase change recorded at a depth $x = 1\ cm$ for three different values of ΔT.

that ΔT is proportional to h [7] ($\Delta T = kh$) where h is the mesh size and k is a constant chosen in a way to obtain good accuracy with fewer fluctuations in the temperature profile. The value of ΔT that insure accuracy of the solution with few fluctuations is called $\Delta T_{optimum}$. The choice of the value of $\Delta T_{optimum}$ is heuristic and was based on numerical trials ($\Delta T_{optimum} = 1000\,h$).
Figure 2 which represents the zoom of temperature profile close to the phase change region for 3 different values of ΔT shows that a smaller value of ΔT ($\frac{\Delta T}{\Delta T_{optimum}} = \frac{1}{4}$) leads to significant fluctuations while an average value ($\frac{\Delta T}{\Delta T_{optimum}} = 1$) will lead to moderate fluctuations whereas for a relatively large value of ΔT ($\frac{\Delta T}{\Delta T_{optimum}} = 4$), the fluctuations disappear but the numerical solution obtained is far from the reference solution. The value of ΔT and its effect on the convergence problem is studied in section 3.8.

2.2 Numerical strategy

We need to solve the heat diffusion equation (PDE) so we choose the method of lines which is a way of approximating PDEs by ODEs where space and time discretizations are considered separately. The spatial discretization is performed using the vertex-centered finite volume method which conserves the mass locally and preserves continuity of fluxes. To apply the spatial discretization, the computational domain is divided into a finite volume grid or mesh with equal length $h = \Delta x$.
In fact, the spatial variable is discretized into N discretization points and each state variable T is transformed into N variables corresponding to its value at each discretization point. It is important to mention that the end points of each interval ($x_{i-\frac{1}{2}}$ and $x_{i+\frac{1}{2}}$) are computed as exactly the middle of two consecutive nodes, i.e. $x_{i+\frac{1}{2}} = \frac{1}{2}(x_i + x_{i+1})$ The spatial derivatives are approximated by using a finite volume formula on three points so we end up with a semi-discrete system of ODEs which can be written in the form:

$$\frac{dT}{dt} = \mathbf{B}(T)T \tag{9}$$

The ODE coefficient matrix $\mathbf{B}(T)$ has a tridiagonal structure due to the 1-D Laplacian discretization. Some tries showed that our ODE system becomes more and more stiff as h becomes smaller. The difficulty with stiff problems is the prohibitive amount of computer time required for their solution by classical ODE solution methods, such as the popular explicit Runge-Kutta and Adams methods. The reason is the excessively small step sizes that these methods must use to satisfy stability requirements due to the high non-linearity of the apparent capacity of the fluid C_f (equation (6)). For this reason, we use an implicit ODE solver (Backward Differentiation Formula) which possesses the property of stability and therefore does not suffer from the stability step size constraint. The BDF implicit scheme requires the calculation of a Jacobian matrix which is calculated and generated by a Computer Algebra System (Maple or Maxima) and then stored in a sparse format. Note that the numerical calculation is performed with `ddebdf` routine of the SLATEC Fortran library which was modified to use the UMFPACK sparse linear solver. The ODE solver performs time integration by adjusting automatically the time step in the BDF scheme and all these primary libraries are grouped in the easy-to-use MUESLI library [10].

3 Inverse problem

In order to solve the parametric inverse problem consisting of finding the volumetric heat capacity $(\rho C)_s$, the conductivity λ_s and the porosity ϕ of the saturated soil, it is necessary to know the values of temperature T_{gi}^f at selected points (sensors) of the porous medium domain for times t^f: $T_{gi}^f = T_g(x_i, t^f)$ where $i = 1,2,...,M$ and $f = 1,2,...,F$. M and F are the total number of sensors and time steps respectively. We use the least squares criterion to solve this inverse problem so we try to find the soil parameters that minimize the error function which is defined by:

$$S((\rho C)_s, \phi, \lambda_s) = \frac{1}{2}\|T_i^f - T_{gi}^f\|_2^2 \tag{10}$$

where $T_i^f = T(x_i, t^f)$ are the temperatures being the solution of the direct problem for the assumed set of parameters at the point x_i, $i = 1,2,...,M$ for the time t^f, $f = 1,2,...,F$ and T_{gi}^f is the measured temperature at the same point x_i for time t^f. It is important to mention that the authors in [2] calculated the temperature at the final time only and at all the points of the domain.

3.1 Parameter scaling

In [2], the authors mentioned that the heat equation is not sensitive to the heat capacity in comparison to the other parameters and that it stagnate at its initial guess. In reality, it is due to the fact that the parameters we are investigating are of very different magnitudes so it is necessary to perform parameter scaling or otherwise many searches would not converge. Gradient search techniques generally require parameter scaling to obtain efficient search convergence [4].

The first basic rule of scaling is that the variables of the scaled problem should be of similar magnitude and of order unity in the region of interest. If typical values of the variables are known, a problem can be transformed so that the variables are all of the same order of magnitude. The most commonly used transformation is of the form :

$$p = \mathbf{D}\tilde{p} \tag{11}$$

where p is the vector of original variables p_j, $\tilde{p}$ is the vector of scaled variables $\tilde{p_j}$ and $\mathbf{D}$ is a constant diagonal matrix whose diagonal elements are set to be equal to the order of magnitude of its corresponding variable. We have to keep in mind that when the variables are scaled then the derivatives of the objective function are also scaled [4].

3.2 Method of resolution

To illustrate the method of resolution, we define the following vectors:

$$T_g = \begin{pmatrix} T_{g1}^1 \\ \dots \\ T_{g1}^F \\ \dots \\ T_{gM}^1 \\ \dots \\ T_{gM}^F \end{pmatrix} \quad g(p^{(k)}) = \begin{pmatrix} T_1^{1,(k)} \\ \dots \\ T_1^{F,(k)} \\ \dots \\ T_M^{1,(k)} \\ \dots \\ T_M^{F,(k)} \end{pmatrix} \quad p^{(k)} = \begin{pmatrix} (\rho C)_s^{(k)} \\ \lambda_s^{(k)} \\ \phi^{(k)} \end{pmatrix}$$

and

$$r(p^{(k)}) = g(p^{(k)}) - T_g$$

where $r(p^{(k)})$ is the residual vector at the iteration k and $N = M \times F$. In [2], the authors used the Gauss-Newton method to solve the nonlinear least square problem which fails to converge in our case when the temperature is calculated at few sensors only but for the whole simulation time due to some lack of information. Moreover, Gauss-Newton method is not locally convergent on problems that are very non-linear or have very large residuals which is the case in our problem. Since the performance of the Gauss-Newton method is strongly dependent on the residual size, we adopted the use of the Damped Gauss Newton method which is an improved version of the Gauss-Newton algorithm [4]. Damped Gauss-Newton method is known to be locally convergent on almost all nonlinear least squares problems including large residual or very nonlinear problems [5].

The cost function $S((\rho C)_s, \phi, \lambda_s)$ defined by equation (10) can be re-written as:

$$S(p^{(k)}) = \frac{1}{2} r(p^{(k)})^T r(p^{(k)}) \tag{12}$$

Such necessary condition for the minimization of $S(p^{(k)})$ can be represented in equation (13):

$$\nabla S(p^k) = \mathbf{J}^T(p^k) r(p^k) = 0 \tag{13}$$

where $J(p^k)_{i,j} = \dfrac{\partial r_i(p^k)}{\partial p_j^k}$, $i = 1,2,...,N$ and $j = 1,2,3$.

The sensitivity matrix, $\mathbf{J}(p^k)$ is defined by:

$$\mathbf{J}(p^{(k)}) = \begin{pmatrix} W_1^{1,(k)} & R_1^{1,(k)} & Z_1^{1,(k)} \\ \dots & \dots & \dots \\ W_1^{F,(k)} & R_1^{F,(k)} & Z_1^{F,(k)} \\ \dots & \dots & \dots \\ W_M^{1,(k)} & R_M^{1,(k)} & Z_M^{1,(k)} \\ \dots & \dots & \dots \\ W_M^{F,(k)} & R_M^{F,(k)} & Z_M^{F,(k)} \end{pmatrix} \tag{14}$$

The elements of the sensitivity matrix are called the Sensitivity Coefficients. The sensitivity coefficient $J_{i,j}^f$ is thus defined as the first derivative of the estimated temperature at position i and time f with respect to the unknown parameter p_j [11], that is,

$$J_{i,j}^f = \frac{\partial T_i^f}{\partial p_j} \tag{15}$$

where $W_i^{f,(k)} = \dfrac{\partial T_i^f}{\partial (\rho C)_s}\Big|_{(\rho C)_s = (\rho C)_s^{(k)}}$, $R_i^{f,(k)} = \dfrac{\partial T_i^f}{\partial \phi}\Big|_{\phi=\phi^{(k)}}$ and $Z_i^{f,(k)} = \dfrac{\partial T_i^f}{\partial \lambda_s}\Big|_{\lambda_s=\lambda_s^{(k)}}$. The Damped Gauss Newton algorithm iteratively finds the minimum of S. Starting with an initial guess $p^{(0)}$ for the minimum, the method proceeds by the iterations:

$$p^{(k+1)} = p^{(k)} + m^{(k)} \tag{16}$$

$m^{(k)}$ is called the increment vector and is defined by:

$$m^{(k)} = -\alpha_k \left[\mathbf{J}(p^{(k)})^T \mathbf{J}(p^{(k)}) \right]^{-1} \mathbf{J}(p^{(k)})^T r(p^k) \tag{17}$$

α_k is the damping parameter ($0 < \alpha_k \leq 1$). An optimal value of α_k could be obtained using a line search algorithm [4]; in our case, we used trial and error to find a suitable constant damping parameter.

3.3 Governing Equations

In the following, we present the heat equation together with the three sensitivity equations resulting from the differentiation of the heat diffusion equation (1) with respect to the soil parameters p_j in 1D coordinate system.

$$\frac{\partial}{\partial p_j}\left[(\rho C)_e \frac{\partial T}{\partial t}\right] = \mathrm{div}\left(\frac{\partial}{\partial p_j}\left[\lambda_e \nabla T\right]\right) \tag{18}$$

which leads to the general sensitivity equation below:

$$(\rho C)_e(T)\frac{\partial U_j(x,t)}{\partial t} + \frac{d(\rho C)_e(T)}{dp_j}\frac{\partial T(x,t)}{\partial t} = \mathrm{div}\left(\lambda_e(T)\nabla U_j(x,t)\right) + \mathrm{div}\left(\frac{d\lambda_e(T)}{dp_j}\nabla T(x,t)\right) \tag{19}$$

where $U_j = \partial T/\partial p_j$. The general sensitivity equation is accompanied with the following boundary and initial conditions:

$$\text{At } t=0: \quad U_j(x,0) = U_{j0} = 0 \quad \text{in } \Omega$$

$$\text{At } x=0: \quad U_j(x,t) = 0 \quad \text{for } t \in (0, t_{end}] \text{ (Dirichlet)}$$

$$\text{At } x=l: \quad \frac{\partial U_j(x,t)}{\partial x} = 0 \quad \text{for } t \in (0, t_{end}] \text{ (Neumann)}$$

3.3.1 Elimination of the approximation used by [2]

In order to determine the sensitivity coefficients (W, R and Z) appearing in the sensitivity matrix, we must solve the three sensitivity equations without using the approximation:

$$\mathrm{div}\left(\lambda_e \nabla T\right) \approx \lambda_e \,\mathrm{div}\left(\nabla T\right) \tag{20}$$

used by [2] and which allowed the authors to write:

$$\frac{(\rho C)_e}{\lambda_e}\frac{\partial T}{\partial t} = \mathrm{div}\left(\nabla T\right) \tag{21}$$

This approximation leads to an approximated sensitivity matrix (Jacobian) and thus the problem needs more iterations to reach the required solution. Differentiating (in 1D) with respect to $(\rho C)_s$, ϕ and λ_s respectively:

$$\frac{\partial W}{\partial t} + \frac{1}{(\rho C)_e}\left[\phi\rho_f\left[(C_v - C_l)\frac{d\sigma}{dT} + L\frac{d^2\sigma}{dT^2}\right]W + \phi C_f(\rho_v - \rho_l)\frac{d\sigma}{dT}W + (1-\phi)\right]\frac{\partial T}{\partial t} - \frac{1}{(\rho C)_e}\frac{\partial}{\partial x}\left(\lambda_e\frac{\partial W}{\partial x}\right) - \frac{1}{(\rho C)_e}\frac{\partial}{\partial x}\left[\frac{\phi\lambda_s^2\frac{d\lambda_f}{dT}}{(\phi\lambda_s + (1-\phi)\lambda_f)^2}W\frac{\partial T}{\partial x}\right] = 0 \tag{22}$$

$$\frac{\partial R}{\partial t} + \frac{1}{(\rho C)_e}\left[(\rho C)_f - (\rho C)_s + \phi\rho_f\left[(C_v - C_l)\frac{d\sigma}{dT} + L\frac{d^2\sigma}{dT^2}\right]R + \phi C_f(\rho_v - \rho_l)\frac{d\sigma}{dT}R\right]\frac{\partial T}{\partial t} - \frac{1}{(\rho C)_e}\frac{\partial}{\partial x}\left(\lambda_e\frac{\partial R}{\partial x}\right) - \frac{1}{(\rho C)_e}\frac{\partial}{\partial x}\left[\frac{E}{(\phi\lambda_s + (1-\phi)\lambda_f)^2}\frac{\partial T}{\partial x}\right] = 0 \tag{23}$$

where

$$E = \left(\lambda_s\frac{d\lambda_f}{dT}\frac{dT}{d\phi}\right)(\phi\lambda_s + (1-\phi)\lambda_f) - \left(\lambda_s - \lambda_f + (1-\phi)\frac{d\lambda_f}{\partial T}\frac{\partial T}{d\phi}\right)\lambda_f\lambda_s$$

$$\frac{\partial Z}{\partial t} + \frac{1}{(\rho C)_e}\left[\phi\rho_f\left[(C_v - C_l)\frac{d\sigma}{dT} + L\frac{d^2\sigma}{dT^2}\right]Z + \phi C_f(\rho_v - \rho_l)\frac{d\sigma}{dT}Z\right]\frac{\partial T}{\partial t} - \frac{1}{(\rho C)_e}\frac{\partial}{\partial x}\left(\lambda_e\frac{\partial Z}{\partial x}\right) - \frac{1}{(\rho C)_e}\frac{\partial}{\partial x}\left(\frac{F}{[\phi\lambda_s + (1-\phi)\lambda_f]^2}\frac{\partial T}{\partial x}\right) = 0 \tag{24}$$

where $F = \left[\lambda_s\frac{d\lambda_f}{dT}\frac{dT}{d\lambda_s} + \lambda_f\right][\phi\lambda_s + (1-\phi)\lambda_f] - \left[\phi + (1-\phi)\frac{d\lambda_f}{dT}\frac{\partial T}{\partial\lambda_s}\right]\lambda_f\lambda_s$

These three sensitivity equations (22), (23) and (24) are completed with adequate initial and boundary conditions. W, R and Z are the unknowns of the sensitivity equations and T is the temperature.

3.4 Numerical strategy

The obtained system of coupled equations (heat diffusion equation + 3 sensitivity equations) is a nonlinear system of partial differential equations. To solve this system, we use the same numerical strategy used in the forward problem (method of lines + finite volume method). After spatial discretization, the system of coupled equations can be written in the form:

$$F(t, Y, Y') = 0 \text{ with } Y(t_0) = Y_0 \tag{25}$$

where $Y = (T\ W\ R\ Z)^T$. The system in equation (25) can be solved by an ODE solver as in the forward problem.

3.5 Algorithm

The aim of the inverse problem is the calculation of the vector parameters p that minimizes the cost function S presented in equation (10). The Damped Gauss Newton (DGN) algorithm that we chose to apply to our nonlinear least square problem is as follows:

1- Choose a constant damping parameter α ($0 < \alpha \leq 1$).
2- Choose an initial value $p^{(0)}$; initialize the iteration $k = 0$
3- Perform the parameters' scaling to obtain $\tilde{p}$;
4- Solve the system (heat equation with phase change + sensitivity equations) using $\tilde{p}^{(k)}$ to define the parameters of the soil. The equivalent parameters of the system are calculated by the apparent heat capacity method (AHC);
• deduce $T_i^{f,(k)}$, $\tilde{W}_i^{f,(k)}$, $\tilde{R}_i^{f,(k)}$ and $\tilde{Z}_i^{f,(k)}$ for $i = 1,...,M$ and $f = 1,...,F$
5- Calculate $r^{(k)}$ and the Sensitivity matrix $\tilde{\mathbf{J}}$ knowing that $\tilde{\mathbf{J}} = \mathbf{J}.\mathbf{D}$
6- Solve the linear system $\tilde{\mathbf{J}}(\tilde{p}^{(k)})^T\tilde{\mathbf{J}}(\tilde{p}^{(k)})\tilde{p}^{(k+1)} = \tilde{\mathbf{J}}(\tilde{p}^{(k)})^T\tilde{\mathbf{J}}(\tilde{p}^{(k)})\tilde{p}^{(k)} - \alpha.\tilde{\mathbf{J}}(\tilde{p}^{(k)})^T r^{(k)}$ for $\tilde{p}^{(k+1)}$.
7- If the criteria of convergence are reached, end.
Calculate the original parameters' vector $p^{(k+1)} = \mathbf{D}.\tilde{p}^{(k+1)}$.
If not, iterate:
$\tilde{p}^{(k)} \leftarrow \tilde{p}^{(k+1)}$ and go to 4.

3.6 Stopping criteria

Classically, there are three convergence tests used in the algorithms for nonlinear least square problems. We chose to apply only two of them. The first test is the X-convergence which is based on an estimate of the distance between the current approximation x and the previous solution x* of the problem. If $\mathbf{D}$ is the current scaling matrix, then this convergence test attempts to guarantee that:

$$\|\mathbf{D}(x - x^*)\| \leq XTOL.\|\mathbf{D}\,x^*\| \tag{26}$$

where XTOL is a user supplied tolerance (we used XTOL = 10^{-6}). The second test, the main convergence test, is based on an estimate of the distance between the Euclidean norm $\|F(x)\|$ of the residuals at the current approximation x and the previous value $\|F(x^*)\|$ at the previous solution x* of the problem. This convergence test (F-convergence) attempts to guarantee that:

$$\|F(x)\| \leq (1 + FTOL).\|F(x^*)\| \tag{27}$$

where FTOL is another user-supplied tolerance (we used FTOL = 10^{-6}).

3.7 Code validation

The code validation is based on choosing a plausible example where the soil parameters $\{(\rho C)_s, \phi, \lambda_s\}$ are given constant values. These values are used by the forward problem to calculate the temperature at 5 different positions of the domain (5 sensors at the depths $x = 1$ *cm*, $x = 2$ *cm*, $x = 3$ *cm*, $x = 4$ *cm* and $x = 5$ *cm* respectively). These temperatures are recorded every 24 seconds for 4 hours. In tables 1 and 2, we used the same number of mesh cells in the forward problem (to create the synthetic data) and in the inverse problem. In both tables, we removed the approximation (see equation (20)). In table 1, we did not use the scaling technique while we used it in table 2. The results presented in the two tables prove that scaling is an important factor to obtain the desirable results.

On the other hand, if we use scaling together with the approximation (20) then we will obtain approximately the same results as those in table 2 but the number of iterations is very large (see figure 3). The figures that represent the remaining parameters are similar to figure 3. The target of our work is to perform a numerical simulation that is the closest possible to the real experimental case. For this reason, we generate the synthetic data using a very large number of mesh cells (around 6000) to obtain accurate results. Thereafter, these data play the role of the experimental data in the inverse problem which is run using small number of mesh cells (40, 80, 120, 160 ...). Figure 4 represents the variation of the final residue as function of the number of mesh cells. We can easily notice that the residue decrease as number of mesh cells increase which assures the consistency of our method. Figure 5 represents the convergence of the conductivity for 120 mesh cells in the inverse problem (the figures representing the convergence of the volumetric heat capacity and porosity are similar). We notice that convergence is achieved after few tens of iterations (37 in this case).

Table 1. Physical properties of the soil obtained by inverse problem **without** scaling (19 iterations).

	$(\rho C)_s$ (J/m^3K)	λ_s (W/m.K)	ϕ
exact	1.95×10^6	0.756	0.20
initial guess	2×10^6	0.8	0.18
calculated	2×10^6	0.7696	0.1979

Table 2. Physical properties of the soil obtained by inverse problem **with** scaling (31 iterations).

	$(\rho C)_s$ (J/m^3K)	λ_s (W/m.K)	ϕ
exact	1.95×10^6	0.756	0.20
initial guess	2×10^6	0.8	0.18
calculated	1.9497×10^6	0.7559	0.2000

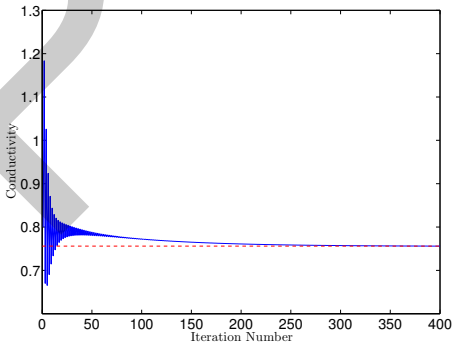

Fig. 3. Variation of λ_s as function of iteration number (using scaling and approximation 20). The red line represents the exact value of λ_s.

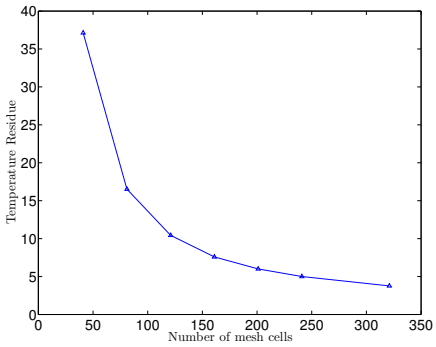

Fig. 4. Variation of residue as function of number of mesh cells. The method is consistent (the error decreases as number of mesh cells increase).

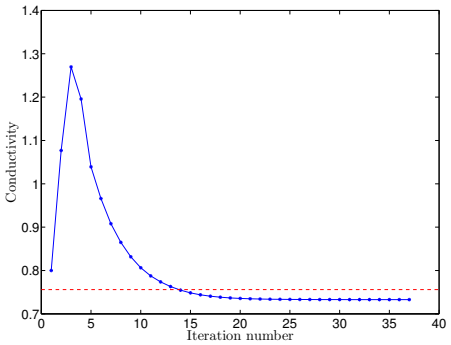

Fig. 5. Variation of the conductivity as function of iteration number. The red line represents the exact value of λ_s.

3.8 Role of ΔT

As we have seen earlier (figures 1 and 2), the choice of the phase change temperature interval ΔT in the AHC method affects the temperature profile. Recall that ΔT is proportional to h [7] ($\Delta T = kh$) where h is the mesh size and k is a constant chosen in a way to obtain good accuracy with fewer fluctuations in the temperature profile. As a consequence, the value of ΔT plays an important role in the results of the inverse problem. If the initial values of parameters are far from the exact solution then the damped Gauss Newton method might not converge using the optimal value of ΔT (see subsection 2.1). To study the effect of this important parameter, we chose the example chosen earlier $\{(\rho C)_s = 1.95 \times 10^6,\ \phi = 0.2,\ \lambda_s = 0.756\}$ and we run the inverse problem using different values of ΔT with 120 as number of mesh cells. We notice that the inverse program fails to converge for $\frac{\Delta T}{kh} = 1$ or 2 and when $\frac{\Delta T}{kh} \geq 11$ whereas it converges for $3 \leq \frac{\Delta T}{kh} \leq 10$. We notice that the values of $(\rho C)_s$, ϕ and λ_s recede from the exact solution and the value of residue increases from 9.588 to 26.7198 as the value ΔT increases from $3 \times \Delta T_{optimum}$ to $10 \times \Delta T_{optimum}$ (see table 3). The results in table 3 are obtained by using $(\rho C)_s = 3 \times 10^6$, $\lambda_s = 0.4$ and $\phi = 0.12$ as initial guesses. If the results obtained in the first row ($\Delta T = 3 \times \Delta T_{optimum}$) are used as initial guesses then the inverse problem will converge to the exact values using $\Delta T_{optimum}$ if we use the same mesh size in both the forward and inverse problems and toward acceptable values if we use huge mesh size to generate the synthetic data and 120 mesh cells in the inverse problem (check table 4).

Table 3. Values of soil parameters and residue obtained by varying $\frac{\Delta T}{kh}$. Results become less accurate as $\frac{\Delta T}{kh}$ increases.

$\frac{\Delta T}{kh}$ \ Soil parameter	$(\rho C)_s$	λ_s	ϕ	residue
3	1.149×10^6	0.5362	0.2319	9.5889
4	8.654×10^5	0.4748	0.2436	11.5282
5	6.42×10^5	0.4306	0.2526	13.5174
7	3.351×10^5	0.3770	0.2640	18.0604
10	6.159×10^4	0.3400	0.2724	26.7198

We call this technique of solving the inverse problem using different values of ΔT over two or more steps, the technique of chaining the inverse problem. This technique works well due to the fact that the fluctuations disappear when we increase the value of ΔT.

Table 4. Physical properties of the soil obtained by inverse problem using $\Delta T = \Delta T_{optimum}$ using the calculated values in table 3 as initial guesses (40 iterations).

	$(\rho C)_s$ (J/m^3K)	λ_s (W/m.K)	ϕ
exact	1.95×10^6	0.756	0.20
initial guess	1.1493×10^6	0.5362	0.2319
calculated	1.9387×10^6	0.7328	0.2001

4 Levenberg Marquardt Algorithm

In section 3, we explained that our inverse problem can be viewed as a nonlinear least square minimization problem which is solved by the Damped Gauss Newton Algorithm. In this section, we present a more robust algorithm to solve the nonlinear least square minimization problem known as Levenberg Marquardt Algorithm (LMA). LMA is the most widely used optimization algorithm for the solution of nonlinear least square problems. It outperforms simple gradient descent and other conjugate gradient methods in a wide variety of problems. It is a blend of original gradient descent and Damped Gauss Newton iteration.

4.1 Introduction to LMA

Levenberg and Marquardt proposed a very elegant algorithm for the numerical solution of equation (10). However, most implementations are either not robust, or do not have a solid theoretical justification. Moré [12] presented a robust and efficient implementation of a version of the Levenberg-Marquardt and show that it has strong convergence properties. In addition to robustness, the main features of this implementation are the proper use of implicitly scaled variables and the choice of the Levenberg-Marquardt parameter. The

implementation of LMA by Moré that is contained in Minpack has proven to be very successful in practice. Several factors make LMA preferable to DGN: first is that LMA possesses an embedded scaling technique, second it is well defined even when J doesn't have full column rank and finally is that when the Gauss-Newton step is too long, the Levenberg Marquardt step is close to being in the steepest-descent direction $-J^T r$ and is often superior to the DGN step. We use the LMDER1 Minpack subroutine for numerical solution of nonlinear least square problems. LMDER1 is based on Moré's LMA version where the user must provide a subroutine to calculate the functions r_1, r_2, ... r_m and the Jacobian matrix $\frac{\partial r_i(p)}{\partial p_j}$. LMDER1 follows the convergence criteria mentioned in section 3.6.

4.2 Applying LMA on our Inverse Problem: Results

Using the LMDER1 Minpack subroutine (which is embedded in the easy-to-use MUESLI library [10]) and providing the Jacobian matrix, we obtain the results summarized in tables 5 and 6 which corresponds to different initial guesses. The Jacobian matrix is calculated using Maple.

Table 5. Physical properties of the soil obtained by inverse problem using LMA. Scaling is used implicitly and approximation (20) is removed. Same number of mesh cells is used in both the forward and inverse problems.

	$(\rho C)_s$ (J/m^3K)	λ_s (W/m.K)	ϕ
exact	1.95×10^6	0.756	0.20
initial guess	2.0×10^6	0.8	0.18
calculated(11 iterations)	1.957×10^6	0.758	0.1996

Table 6. Same legend as table 5.

	$(\rho C)_s$ (J/m^3K)	λ_s (W/m.K)	ϕ
exact	1.95×10^6	0.756	0.20
initial guess	2.5×10^6	0.4	0.16
calculated (10 iterations)	1.958×10^6	0.758	0.1996

We notice that even if the initial values are changed the parameters converge to the same exact values.

In figures 6, 7, 8 and 9 which correspond to table 5, we notice that the calculated values of the parameters are very close to the exact ones and that the residue approaches zero due to the fact that we used same number of mesh cells in both direct and inverse problems.

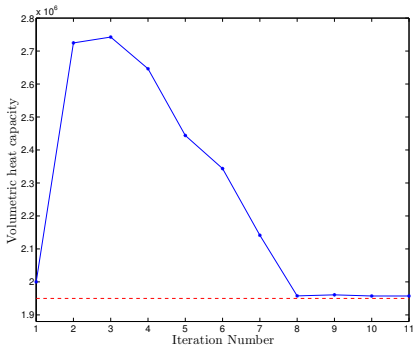

Fig. 6. Variation of the volumetric heat capacity as function of iteration number using LMA (Same number of mesh cells in both the forward and inverse problems). The red line represents the exact value of $(\rho C)_s$.

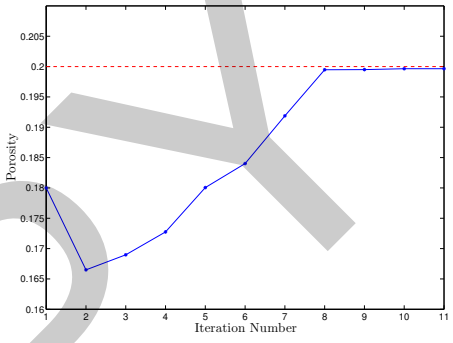

Fig. 7. Variation of the porosity as function of iteration number using LMA (Same number of mesh cells in both the forward and inverse problems). The red line represents the exact value of ϕ.

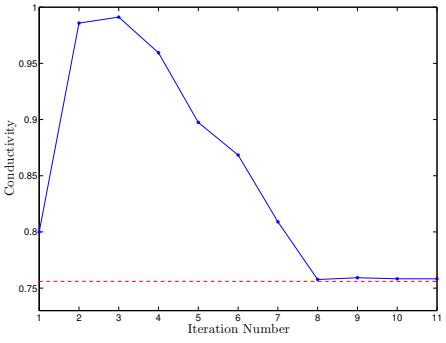

Fig. 8. Variation of the conductivity as function of iteration number using LMA (Same number of mesh cells in both the forward and inverse problems). The red line represents the exact value of λ_s.

4.3 Sensitivity Analysis

Sensitivity analysis can split model parameters in two sets: sensitive and insensitive parameters. To study the sensitivity of the parameters in our model, we use the method discussed in [13] where the authors use singular value decomposition of the sensitivity matrix J followed by QR factorization to determine whether the parameters are sensitive or not and the order od sensitivity. For example, in the study analyzed here we used an ODE solver with an absolute error tolerance of 10^{-6} , i.e., the error of the numerical model solution is of order 10^{-6} and the error in the Jacobian matrix is approximately $\sqrt{10^{-6}} = 10^{-3}$. Consequently, for an identifiable

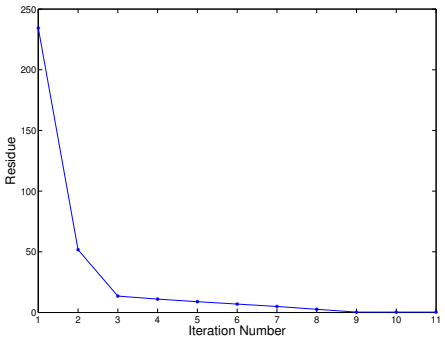

Fig. 9. Variation of the residue as function of iteration number using LMA (Same number of mesh cells in both the forward and inverse problems).

parameter, the singular value must be greater than 10^{-3}. The singular values of our sensitivity matrix are $\sigma_1 = 4.86 \times 10^3$, $\sigma_2 = 4.24 \times 10^2$ and $\sigma_3 = 26.79$. This means that the 3 parameters are identifiable. Applying a QR decomposition with column pivoting, we deduce that ϕ is the most identifiable parameter then λ_s and finally $(\rho C)_s$.

5 Conclusion

The idea of this paper was the enhancement of the inverse problem presented in [2] using a more realistic approach where we estimate the thermophysical properties of the soil knowing the temperature history at selected points of the domain (few sensors). In order to solve this inverse problem, we used the least square criterion where we try to minimize the error function between synthetic measures and calculated ones. The coupled system composed of the energy equation together with the three sensitivity boundary initial value problems resulting from differentiating the basic energy equation with respect to the soil properties must be solved. To overcome the stiffness of our problem (due to the use of AHC method), the high nonlinearity of the coupled system and the problem of large residuals we used the Damped Gauss Newton and Levenberg-Marquardt methods. Our model is strongly similar to the experimental setup in laboratory so real experimental data could replace the synthetic data but to obtain accurate results a relatively small mesh size must be used which will lead to a high numerical cost. In addition, our configuration has the advantage that all soil parameters including the volumetric heat capacity converges to the required exact solution which was not the case in any previous work since we adopted a variable-scaling technique and we removed the approximation (see equation (20)) which leads to an exact sensitivity matrix (Jacobian) and thus reducing the number of iterations till convergence. Moreover, we emphasized on the importance of the choice of ΔT where for a certain initial guess the inverse problem fails to converge. We overcome this problem by chaining the inverse problems using different values of ΔT and parameters' set. The method presented in this paper can be easily applied to 2D and 3D configurations.

References

[1] Olandunjoye, M. A., Sanuade, O. A., and Olaojo, A. A., 2013. "Variability of soil thermal properties of a seasonally cultivated agricultural teaching and research farm". *Global Journal of Science Frontier Research Agriculture and Veterinary,* **13**, pp. 40–64.

[2] Muhieddine, M., Canot, É., and March, R., 2012. "Heat transfer modeling in saturated porous media and identification of the thermophysical properties of the soil by inverse problem". *J. Applied Numerical Mathematics,* **62**, pp. 1026–1040. DOI: `http://dx.doi.org/10.1016/j.apnum.2012.02.008`.

[3] Engl, H. W., and Kugler, P., 2005. "Nonlinear inverse problems: theoretical aspects and some industrial applications". *Multidisciplinary Methods for Analysis, Optimization and Control of Complex systems,* **6**, pp. 3–47.

[4] Dennis, J. E., and Schnabel, R. B., 1983. *Numerical methods for unconstrained optimization and nonlinear equations*. Prentice-Hall, INC. New Jersey.

[5] Björck, A., 1990. *Numerical methods for least squares problems*. Siam.

[6] Majchrzak, E., Mochnacki, B., and Suchy, J., 2008. "Identification of substitute thermal capacity of solidifying alloy". *Journal of Theoretical and Applied Mechanics,* **46**(2), pp. 257–268.

[7] Muhieddine, M., Canot, É., and March, R., 2009. "Various approaches for solving problems in heat conduction with phase change". *International Journal on Finite Volumes,* **6**(1), pp. 1–20.

[8] Bonacina, C., and Comini, G., 1973. "Numerical solution of phase-change problems". *Int. J. Heat Mass Transfer,* **16**, pp. 1825–1832. DOI: `http://dx.doi.org/10.1016/0017-9310(73)90202-0`.

[9] Civan, F., and Sliepcevich, C. M., 1987. "Limitation in the apparent heat capacity formulation for heat transfer with phase change". In proc. Okla. Acad. Sci. 67, pp. 83–88.

[10] Canot, É. *Muesli Reference Manual - Fortran 95 implementation*. Available at `http://people.irisa.fr/Edouard.Canot/muesli`.

[11] Özişik, M. N., and Orlande, H. R. B., 2000. *Inverse heat transfer*. Taylor and Francis.

[12] Moré, J. J., 1978. "The Levenberg-Marquardt algorithm: implementation and theory". *Numerical Analysis, Lecture Notes in Mathematics, Springer, Berlin,* **630**.

[13] Pope, S. R., Ellwein, L. M., Zapata, C. L., Novak, V., Kelley, C. T., and Olufsen, M. S., 2009. "Estimation and identification of parameters in a lumped cerebrovascular model". *Mathematical Biosciences and Engineering,* **6**(1), pp. 93–115.